Chinese Science Bulletin

Short-term exposure of low-alloyed steels in Qinghai Salt Lake atmosphere

LI QiaoXia, WANG ZhenYao†, HAN Wei, YU GuoCai & HAN EnHou

State Key Laboratory for Corrosion and Protection, Institute of Metal Research, Chinese Academy of Sciences, Shenyang 110016, China

The rusts formed on carbon steel and weathering steel exposed in Qinghai Salt Lake atmosphere for 6 months were characterized by X-ray diffraction (XRD), infrared transmission spectroscopy (IRS), scanning electron microscopy (SEM), electron probe micro analyzer (EPMA) and electrochemical polarization techniques. The two kinds of steels showed the similar corrosion rate, corrosion product composition and electrochemical polarization behavior. Their rusts were mainly composed of β-FeOOH, $Fe_8(O,OH)_{16}Cl_{1.3}$ and a little γ-FeOOH. Cl^- played an important role during the corrosion process of low-alloyed steels. The alloyed elements Cr, Ni and Cu in weathering steel were detected in the rusts; however, they showed no remarkable protective ability.

atmospheric corrosion, carbon steel, weathering steel, XRD, EPMA

Carbon steel and weathering steel as important structural materials are widely used in buildings, bridges, towers, and vehicles, etc. These equipments are mainly operated under atmospheric environment. Particles and dust in the air often induce the corrosion of steel and significantly influence its service life[1,2]. Among various atmospheric pollutant particles, chloride ion attracts much attention because it is more readily adsorbed than oxygen in competition for surface sites and severely disrupts the protective nature of the corrosion film on steels[1,2]. In addition, the dissolved chlorides increase the conductivity of the aqueous solution formed at the surface of the steels, resulting in the acceleration of corrosion. Marine atmosphere contains an amount of chlorides and the corrosion behaviors of low-alloyed steels exposed to this environment have been studied[3–5]. Salt lake atmosphere also contains chlorides particles. However, little work has been addressed about the atmospheric corrosion of low-alloyed steels in this kind of environment.

Qinghai Salt Lake is located in the northwest of China. The atmospheric corrosion in this region is aggravated by the high salinity in salt lake water and high rates of natural and sea-salt deposition[6]. With the fast development of local economy, the corrosiveness of the salt lake atmosphere for steels has received more interests. Thus, in this paper, the rusts formed on carbon steel and weathering steel exposed to a salt lake region for 6 months were characterized and the corrosion mechanism was discussed.

1 Experimental

1.1 Exposure tests

Test specimens were cut from commercially available Q235 carbon steel and Corten A weathering steel and their compositions are given in Table 1. The coupons (100 mm×50 mm×5 mm) and electrode samples (exposed area 1 cm^2) were exposed to Qinghai Salt Lake atmospheric environment at an angle of 45° facing south under open conditions for 6 months. The exposure site is on an office building roof which is about 40 m away from the salt lake.

Received July 1, 2008; accepted November 23, 2008; published online May 13, 2009
doi: 10.1007/s11434-009-0026-5
†Corresponding author (email: zhywang@imr.ac.cn)
Supported by the National Natural Science foundation of China (Grant No. 50499331)

Citation: Li Q X, Wang Z Y, Han W, et al. Short-term exposure of low-alloyed steels in Qinghai Salt Lake atmosphere. Chinese Sci Bull, 2009, 54: 3446−3452, doi: 10.1007/s11434-009-0026-5

Table 1 Compositions of carbon steel and weathering steel (wt.%)

Steel	Element								
	C	Si	Mn	P	S	Cr	Ni	Cu	Al
Q235	0.14	0.01	0.33	0.011	0.02	–	–	–	–
Corten A	0.09	0.3	0.35	0.081	0.005	0.48	0.27	0.28	0.037

1.2 Characterization of the rusts

Compositions of the rusts were determined by a Nicolet Corporation Model magna-IR560 (with Veemax accessory) infrared spectrophotometer and a Rigaku-D/max-2500PC Model X-ray diffractometer. The surfaces of rust layers were analyzed by a FEI Company Model XL30 ESEM FEG environmental scanning electron microscopy (ESEM) and energy dispersive analysis of X-rays (EDAX). A Shimadzu Model EPMA-1610 electron probe micro analyzer was employed to investigate the distributions of some important elements in the rust.

1.3 Electrochemical measurements

Potential dynamic polarization measurements were carried out by a Princeton Applied Research (PAR) 263 potentiostat in 0.1 mol/L Na_2SO_4 electrolyte open to the air at (20±1)℃. A three-electrode system was adopted and the reference electrode was a commercial saturated calomel one (SCE). Prior to the measurements, the rusted electrodes were left freely in the solution for 60 min allowing the open-circuit potential to reach a steady state.

2 Results and discussion

2.1 Morphology of the rust layer

All the exposed samples were completely covered by corrosion products after exposure for 6 months. And a relatively uniform dark brown rust layer was developed on the upward and downward surfaces of weathering and carbon steels. After removing corrosion products, the mass loss of the steels was determined and shown in Table 2.

Figure 1 shows the metallographic cross sections of the rusted steel samples. The corrosion products consisted of one layer on every side surface of weathering and carbon steels. The thickness of the rust layers on fifteen different regions of each cross section was measured and averaged. The results are shown in Table 2. Comparing mass loss and rust layer thickness of weathering steel with carbon steel, it could be seen that the corrosion grades of the two kinds of steels were similar. In addition, for the same steel, its upward and downward surfaces exhibited no apparent difference in corrosion degree by the rust layer thickness analysis.

Table 2 Thickness and mass loss analysis results

Steel	Average thickness (μm)		Mass loss (g/m^2)
	upward	downward	
Q235	22	22	66.76
Corten A	23	22	61.85

Figure 2 shows the SEM of the rusted steel surfaces. For each kind of steel, its upward and downward surface had a similar morphology. White and loose clumps in different sizes were scattered in the rust layers. The selected rectangle area of the rust layers in Figure 2 was magnified and displayed in Figure 3. All rust layers contained many microcracks, indicating that the rusts on both kinds of steels could not effectively prevent corro-

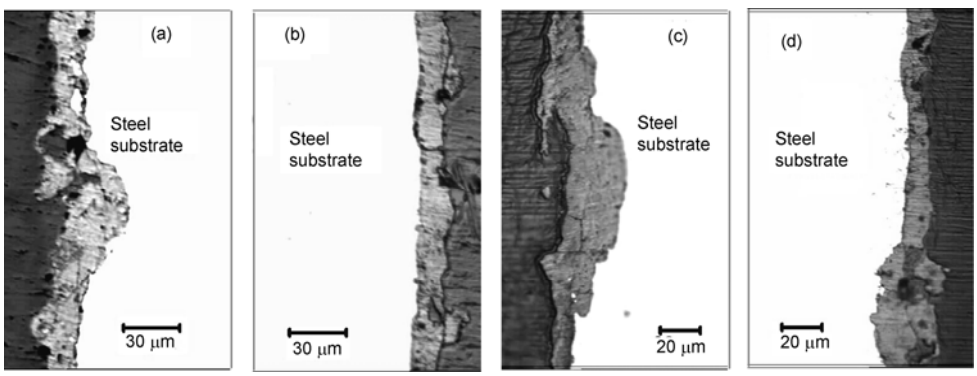

Figure 1 Metallographic cross sections of the rusted samples. (a) Upward surface of carbon steel; (b) downward surface of carbon steel; (c) upward surface of weathering steel; (d) downward surface of weathering steel.

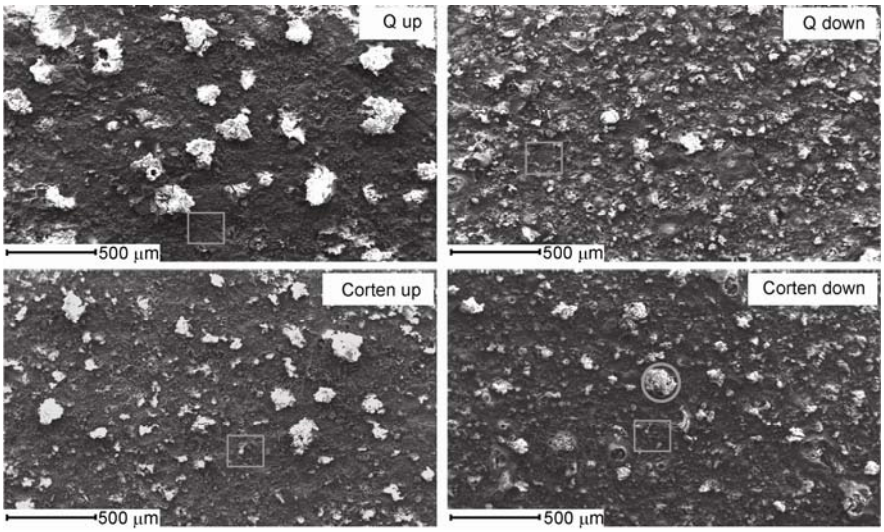

Figure 2 Morphology of the rusted steel surfaces after being exposed in the salt lake atmosphere for 6 months.

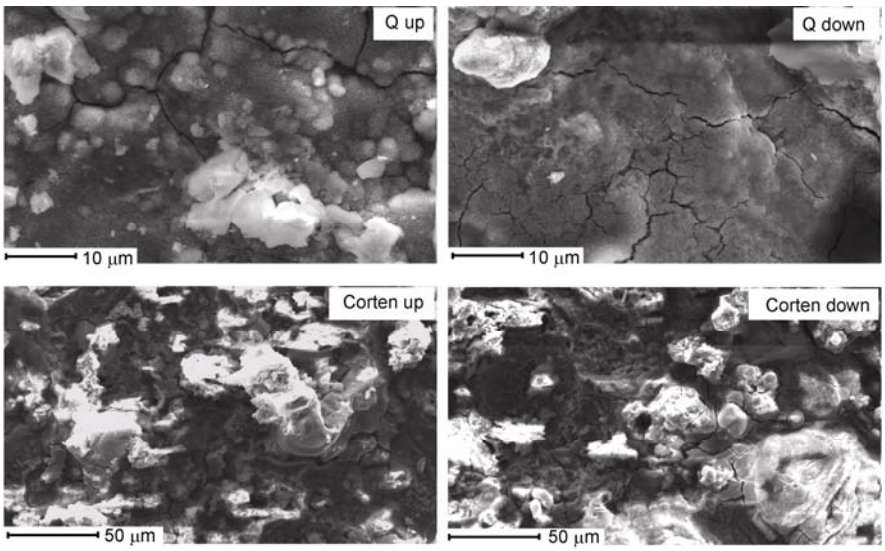

Figure 3 High magnification in the selected rectangle area of the rust layers in Figure 2.

sive chloride ions from contacting the substrate.

More than 10 different points on the clumps covers and the rest areas on each surface were selected and analyzed by EDX. The elements and their average contents were determined and listed in Table 3. O, Mg, S and Cl were found in upward and downward rust layers, whereas Al, Si, K and Ca were detected only in upward rust. The amount of S was little while Cl was rich in the corrosion products. Similar results were also obtained by EPMA analysis of the cross section of the rusts. This illuminated that Cl^-, not S, had an influence on the corrosion of steels in the salt lake area. It can be seen from Table 3 that the content of Cl in the clumps covers was higher than that in the rest areas on each surface. In order to know the distribution details of Cl, a clump was randomly chosen on downward surface of weathering steel (shown with a circle in Figure 2) and five different points (Positions 1—5, from center to the edge) in its area were examined through EDX. The results are shown in Table 4. From center to the edge of the clump, much Cl and Fe were detected and the content of Cl remarkably decreased. Based on the above analysis, it can be concluded that during the initial exposure periods, the formation of compounds containing iron and chlorine accelerated the corrosion of steels.

2.2 Distribution of elements

The distribution of some important elements in the rust layers formed on carbon steel and weathering steel are determined by EPMA and shown in Figures 4 and 5, respectively. The striking feature was rich Cl and poor S

Table 3 Element content (wt.%) in the rusts on the upward and downward surfaces of two kinds of steels

Element	On clumps of Q235		On rest area of Q235		On clumps of Corten A		On rest area of Corten A	
	upward	downward	upward	downward	upward	downward	upward	downward
O	8.57	8.17	5.38	6.94	11.16	11.59	5.92	12.87
Mg	1.34	2.16	1.16	1.54	1.32	0.72	1.73	2.05
S	1.12	0.93	0.89	0.80	1.37	0.98	1.03	0.83
Cl	10.74	9.60	4.66	4.73	13.45	9.67	9.39	6.76
Al	1.51	–	1.17	–	5.70	–	1.92	–
Si	2.82	–	2.11	–	9.34	–	8.24	–
K	0.93	–	0.68	–	1.22	–	0.67	–
Ca	1.03	–	1.30	–	1.17	–	0.92	–

Table 4 EDX analysis result of a clump cover on downward surface of Corten A steel in Figure 2 (wt.%)

Element	Position				
	1	2	3	4	5
O	6.75	10.81	8.37	4.86	7.84
Cl	34.78	32.63	12.67	9.91	4.19
Fe	58.47	56.57	78.96	85.23	87.97

in the whole rusts of the two kinds of steels, which is in good agreement with the detected result by SEM/EDX. It is worth noting that a large amount of Mg appeared in the rusts on the two kinds of steels. Airborne $MgCl_2$ particles were deposited on the surface of steels and deliquesced, and Mg^{2+} and Cl^- were released[7]. After further reactions, insoluble compounds of Mg were formed and retained in the rust. On the surfaces of steels, oxygen atoms were distributed at high content in the corrosion products, which were mainly composed of oxyhydroxides and hydroxychlorides of iron (confirmed by the later XRD patterns). Si was detected in the rusts and it was considered that sand particles in the air penetrated and were accumulated in the product[8]. In addition, for weathering steel, Cr, Cu and Ni were observed in the rust layer and Cu and Ni were uniformly distributed. Generally, these three elements were beneficial to improving the resistance of the steel to atmospheric corrosion[4,8]. However, in this work, the mass loss and rust layer thickness of weathering steel were close to those of carbon steel, indicating that the resistant function of the alloyed elements was confined because of the presence of abundant Cl in the rusts. P was not detected since the content of P in Corten A weathering steel is smaller than others reported[4,8].

2.3 Constituent compounds of rust

Figure 6 exhibits the XRD results of the powered corrosion products on upward and downward surfaces of the two kinds of steels. They were mainly composed of β-FeOOH, $Fe_8(O,OH)_{16}Cl_{1.3}$ and a little γ-FeOOH. IR analysis of the rusts (shown in Figure 7) also confirmed

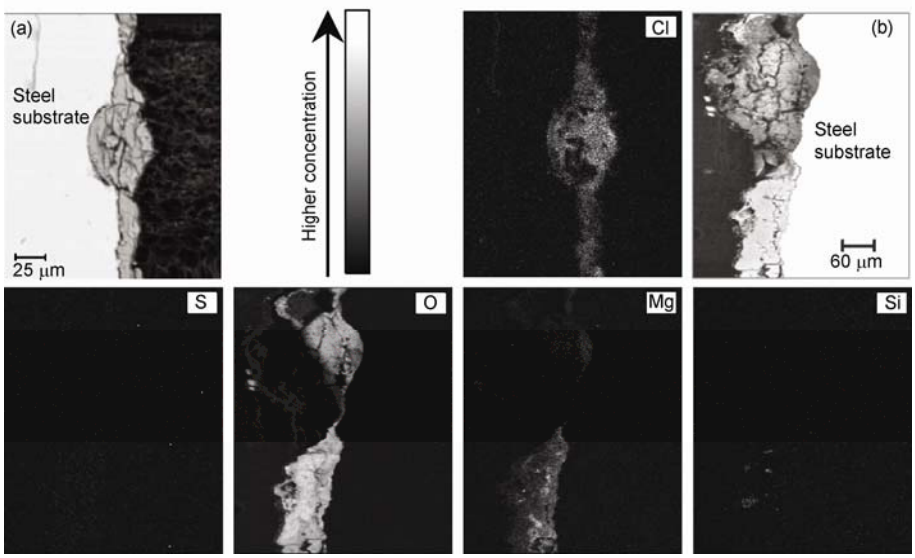

Figure 4 The distribution of Cl, S, O, Mg and Si in the rust formed on upward surface of carbon steel. Back Scatter Electron Image (BSEI) of the analyzed portion is shown in (a) and (b). (a) and (b) are from the same sample.

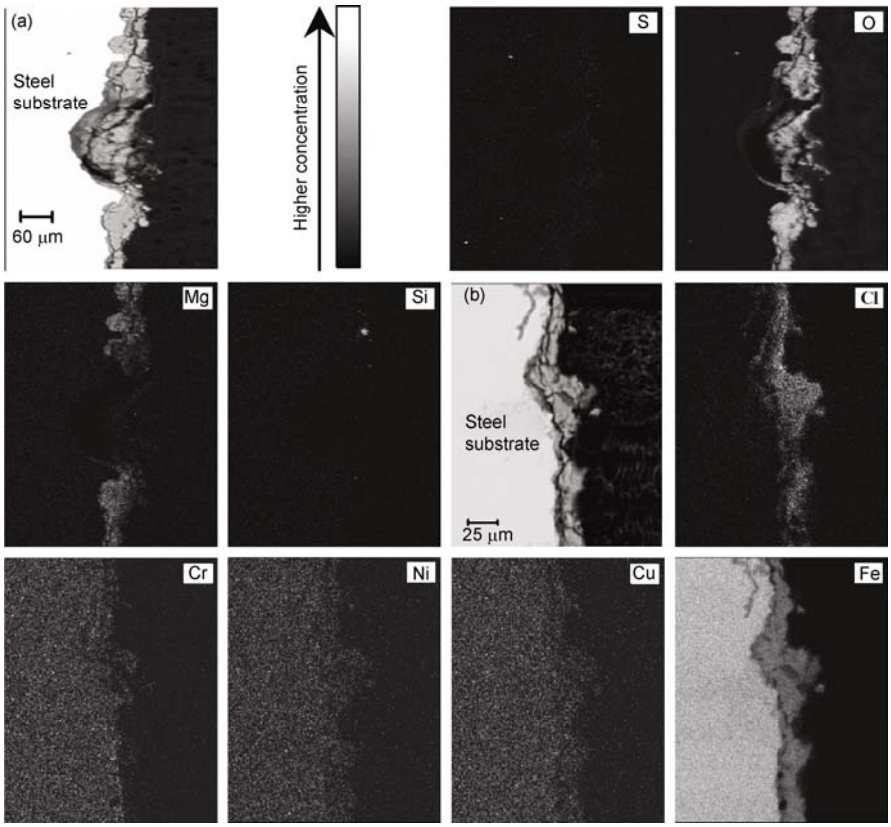

Figure 5 The distribution of S, O, Mg, Si, Cl, Cr, Cu, Ni and Fe in the rust formed on upward surface of weathering steel. Back Scatter Electron Image (BSEI) of the analyzed portion is shown in (a) and (b). (a) and (b) are from the same sample.

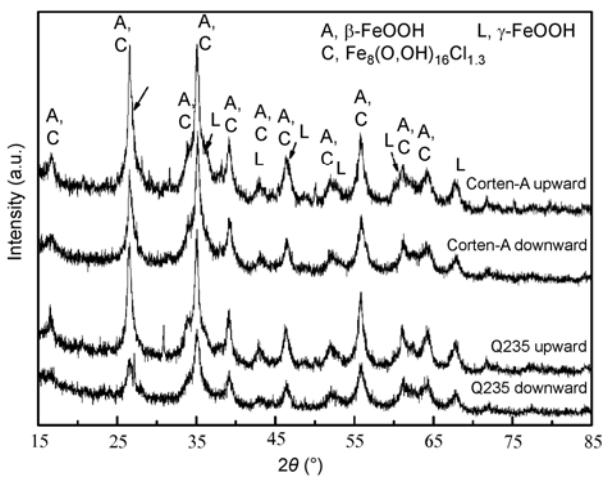

Figure 6 X-ray diffraction patterns of the rusts formed on the upward and downward surfaces of the two kinds of steels.

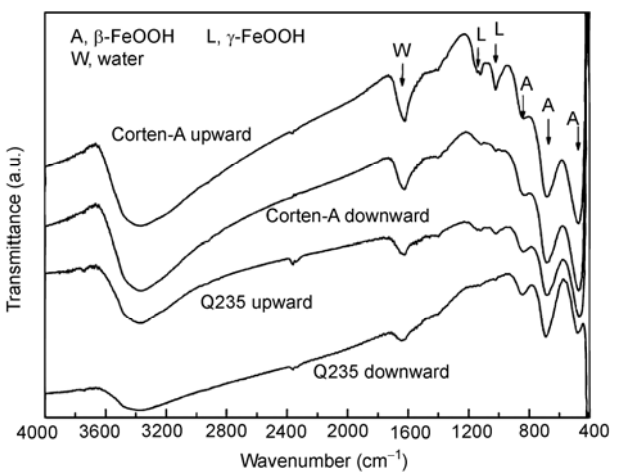

Figure 7 IR spectra of the powdered rust formed on the upward and downward surfaces of the two kinds of steels.

the presence of β-FeOOH and γ-FeOOH. No IR data for $Fe_8(O,OH)_{16}Cl_{1.3}$ could be referenced in literatures. In addition, broader and weaker peaks of γ-FeOOH on downward surfaces of the two kind of steels indicated its poor crystallization. The absorption band at the vicinity of 1630 cm^{-1} demonstrates that a considerable amount of bound water was contained in the corrosion products[8].

2.4 Electrochemical polarization

To evaluate the protectiveness of the rust layers, anodic and cathodic polarization measurements were carried out on different samples and the results are shown in Figure 8. The free corrosion potentials of both kinds of steels were about –0.630 V (SCE).

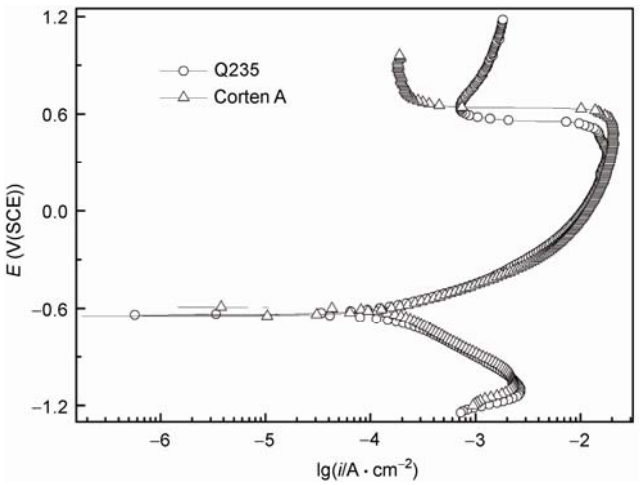

Figure 8 Polarization curves of the rusted electrode samples exposed upwardly.

(i) Anodic polarization. Anodic polarization curves of rusted carbon steel and weathering steel were similar. With the increase of potential from the free corrosion potential to about 0.5 V (SCE), the current densities of two kinds of steels increased exponentially and the values of current densities were very close, indicating the anodic dissolution rate for carbon steel and weathering steel were almost the same and the alloyed elements in weathering steels showed no protective action. This is in good agreement with the results that weight loss and rust layer thickness of two kinds of steels were close (Table 2). As the potential moved to higher potential, the current density greatly decreased and then increased slowly. This may be because the following reaction occurred:

$$Fe^{2+} \rightarrow Fe^{3+} + e \qquad (1)$$

The standard potential of the electrode reaction is 0.53 V (SCE)[9]. In addition, when the potential was larger than 0.65 V (SCE), the current density of weathering steel was smaller in comparison with that of carbon steel, which is because that the alloyed constituents existed in the rusts of weathering steel and their higher valence products blocked the anodic dissolution of the steel[10].

(ii) Cathodic polarization. The cathodic current densities of rusted carbon steel and weathering steel increased rapidly with the decrease of the potential. And the values of their cathodic currents were very large, which was attributed to the reduction of the rust layers[5,11,12]. In addition, the cathodic curves for rusted carbon steel and weathering steel were nearly overlapped, implying that the species in the rusts that were involved in the cathodic reaction were very close. In other words, the two kinds of steels had similar rust composition, which agreed well with the XRD and IR spectra results (Figures 6 and 7).

2.5 Corrosion mechanism

In this work, weathering steel and carbon steel exhibited the similar corrosion rate, corrosion product and polarization behavior. The alloyed element in weathering steel showed no remarkable protective ability due to the short exposure time[8].

Based on all the above analysis, it could be summarized that Cl^- played an important role during the initial corrosion process of carbon steels and weathering steels in Qinghai Salt Lake atmosphere. And the corrosion process involved a micro-cell mechanism[13,14]. At the beginning of exposure, saline particles were deposited on the steel surface and reacted with water in air resulting in the formation of an electrolyte film and the release of chloride ions. At anodic sites that the electrolyte film covered, iron was dissolved and transformed into ferrous ions. At cathodic area that was not covered, O_2 was reduced. The excess positive charge at anodic sites was balanced by chloride ions. In this way, electrochemical cell Fe | $FeCl_n$ solution | O_2 was formed and scattered on the steel surface, which accelerated the corrosion of steel. $FeCl_n$ could deliquesce and a neutral or slightly acidic environment was created, which was unfavorable for the formation of $Fe(OH)_n$[4,7]. In this environment, mixed Fe (II, III) complex hydroxychlorides, such as intermediate product "green rust I" [GRI($Fe(OH,Cl)_{2.55}$)], tended to be formed because iron possessed the ability to be readily transformed between the +2 and +3 valence states[3,5]. These intermediate iron hydroxychlorides were easily oxidized in air and converted into various corrosion products, such as β-FeOOH, $Fe_8(O,OH)_{16}Cl_{1.3}$ and γ-FeOOH. With the formation and accumulation of rust film on steel surface, the cathodic reaction was dominated by the reduction of rusts. In addition, Cl^- penetrated into the rust-metal interface along the cracks and holes in the rust film. The electrochemical cell was changed to Fe | $FeCl_n$ solution | rust and the corrosion was continued.

3 Conclusions

In the early exposure (for 6 months) in salt lake atmosphere, weathering steel and carbon steel showed analogous corrosion behavior. For the same kind of steel, the corrosion degree of upward surface was similar to that of downward surface. The rusts on both kinds of steels

consisted of one layer and were mainly composed of β-FeOOH, $Fe_8(O,OH)_{16}Cl_{1.3}$ and a little γ-FeOOH. Cl^- played an important role in the corrosion of low-alloyed steels and promoted the formation and development of rust layer by the micro-cell mechanism. Cr, Cu and Ni alloyed elements were detected in the rust layer of weathering steel; however, these elements exhibit no apparent protective function.

1 Balasubramanian R. Role of nanophase oxides in short-term atmospheric corrosion of structural steels. Ph.D. Thesis. Norfolk, VA: Old Dominion University, 2003. 4
2 Syed S. Atmospheric corrosion of materials. Emirat J Eng Res, 2006, 11: 1－24
3 Asami K, Kikuchi M. In-depth distribution of rusts on a plain carbon steel and weathering steel exposed to coastal-industrial atmosphere for 17 years. Corros Sci, 2003, 45: 2671－2688[DOI]
4 Misawa T, Kyuno T, Suetaka W, et al. The mechanism of atmospheric rusting and the effect of Cu and P on the rust formation of low alloy steels. Corros Sci, 1971, 11: 35－48[DOI]
5 Nishimura T, Katayama H, Noda K, et al. Electrochemical behaviour of rust formed on carbon steel in a wet/dry environment containing chloride ions. Corrosion, 2000, 56: 935－941
6 Li Q X, Wang Z Y, Han W, et al. Characterization of the rust formed on weathering steel exposed to Qinghai Salt Lake atmosphere. Corros Sci, 2008, 50: 365－371[DOI]
7 Masuda H. Effect of magnesium chloride liquid thickness on atmospheric corrosion of pure iron. Corrosion, 2001, 57: 99－109
8 Yamashita M, Miyuki H, Matsuda Y, et al. The long term growth of the protective rust layer formed on weathering steel by atmospheric corrosion during a quarter of a century. Corros Sci, 1994, 36: 283－299[DOI]
9 Cao C N. Principles of Electrochemical of Corrosion (in Chinese). 2nd ed. Beijing: Chemistry Industry Press, 2004. 329
10 Scharnweber D, Forker W, Rahner D, et al. An electrochemical and surface analytical investigation of weathering steels. Corros Sci, 1984, 24: 67－73[DOI]
11 Suzuki I, Hisamatsu Y, Masuko N. Nature of atmospheric rust on iron. J Electrochem Soc, 1980, 127: 2210－2215[DOI]
12 Matsushima I, Ueno T. On the protective nature of atmospheric rust on low-alloy steel. Corros Sci, 1971, 11: 129－140[DOI]
13 Evans U R, Taylor C A J. Mechanism of atmospheric rusting. Corros Sci, 1972, 12: 227－246[DOI]
14 Evans U R. Mechanism of rusting. Corros Sci, 1969, 9: 813－821[DOI]